General Disclaimer

One or more of the Following Statements may affect this Document

- This document has been reproduced from the best copy furnished by the organizational source. It is being released in the interest of making available as much information as possible.

- This document may contain data, which exceeds the sheet parameters. It was furnished in this condition by the organizational source and is the best copy available.

- This document may contain tone-on-tone or color graphs, charts and/or pictures, which have been reproduced in black and white.

- This document is paginated as submitted by the original source.

- Portions of this document are not fully legible due to the historical nature of some of the material. However, it is the best reproduction available from the original submission.

AN INVESTIGATION ON THE EFFECT OF

SECOND-ORDER ADDITIONAL THICKNESS DISTRIBUTIONS TO

THE UPPER SURFACE OF AN NACA 64_1-212 AIRFOIL

JANUARY 1975

CONTRACT NAS 2-8599

DRAFT

DONALD S. HAGUE

ANTONY W. MERZ

Prepared by

AEROPHYSICS RESEARCH CORPORATION

Bellevue, Washington   98009

TABLE OF CONTENTS

LIST OF ILLUSTRATIONS

ABSTRACT

This report describes a series of low speed airfoil designs based on modifications to the NACA 64_1-212 airfoil. Designs are based on potential flow theory. This report describes one of a series of airfoil modifications carried out under Contract NAS 2-8599, Application of Multivariable Search Techniques to Optimal Wing Design in Non-Linear Flow Fields. Mr. Raymond Hicks of National Aeronautics and Space Administration's Aeronautical Division, Ames Research Center, served as contract monitor for the present study.

AN INVESTIGATION ON THE EFFECT OF

SECOND-ORDER ADDITIONAL THICKNESS DISTRIBUTIONS TO

THE UPPER SURFACE OF AN NACA 64_1-212 AIRFOIL

by Donald S. Hague and Antony W. Merz

Aerophysics Research Corporation

SUMMARY

An investigation has been conducted on the Lawrence Radiation Center, Berkeley, CDC 7600 digital computer to determine the effects of additional thickness distributions to the upper surface of an NACA 64_1-212 airfoil. Additional thickness distributions employed were in the form of two second-order polynomial arcs which have a specified thickness, $\bar{y}$, at a given chordwise location, $\bar{x}$. The forward arc disappears at the airfoil leading edge, the aft arc disappears at the airfoil trailing edge. At the juncture of the two arcs, $x = x$, continuity of slope is maintained. The effect of varying the maximum additional thickness and its chordwise location on airfoil lift coeeficient, pitching moment, and pressure distribution was investigated. Results were obtained at a Mach number of 0.2 with an angle-of-attack of 6° on the basic NACA 64_1-212 airfoil. All calculations employ the full potential flow equations for two dimensional flow. The relaxation method of Jameson is employed for solution of the potential flow equations.

Increases in the rearward location of the maximum additional thickness and increases in the magnitude of the additional thickness both produce increases in the airfoil lift coefficient. Conversely moving the location of maximum thickness forward or decreasing the maximum thickness both reduce the magnitude of the quarter chord pitching moment. The magnitude of the largest pressure peak varies in a complicated manner with maximum additional thickness and its chordwise location. For maximum thickness locations forward of the 2/3 chord additional thickness initially produces a reduction in pressure peak with a lift coefficient increase. With larger amounts of additional thickness pressure peak value and lift

coefficient rise together. For maximum thickness locations aft of the 2/3 chord location additional thickness produces a monotonic rise in both lift coefficient and pressure peak magnitude. A consequence of this behavior is that for a given lift coefficient value the peak pressure can be minimized by careful selection of the location of maximum thickness and its magnitude. Generally as the lift coefficient rises the maximum thickness location moves aft. For a C_L of 1.2 the optimal location for maximum thickness is at the quarter chord. For a C_L of 1.8 the optimal location is approximately at the half chord.

It should be noted that viscous effects are neglected in the present analysis. At the higher lift coefficients the effect of viscosity could be significant. Further investigations incorporating a viscous flow model are therefore desirable.

INTRODUCTION

The National Aeronautics and Space Administration and others are currently conducting a series of theoretical and experimental studies to define airfoil sections having improved performance from the aspects of lift, drag, pitching moment or pressure distribution characteristics, refs 1 and 2. Analytic investigations using airfoil surface representations based on high-order polynomials may result in impractical profiles, for example, very thin trailing edge thickness distributions or severe reflexes in the profile. The present study employs low-order polynomial arcs of second-order whose characteristics are selected to avoid such problems. Optimization studies using multivariable search techniques, reference 3, generally indicate that shape changes which provide increased lift produce unfavorable changes in moment characteristics. Conversely profile changes which improve the moment characteristics decrease the lift coefficient. With the low-order model of the present investigation a systematic examination on the effect of profile changes can be carried out. This was accomplished and the trends revealed by optimization studies were confirmed. An interesting by product of the systematic

investigation of profile changes is that a gain in lift coefficient can be produced while reducing the peak negative pressures. This tends to decrease the pressure gradient and hence holds promise for the development of practical single component high lift coefficient airfoils.

MATHEMATICAL MODELS

Potential Flow Equation

Potential flow analysis is based on solution of the two-dimensional potential flow equation

$$(a^2-u^2) \phi_{xx}+(a^2-v^2) \phi_{yy}-2uv \phi_{xy} = 0$$

where ϕ is the velocity potential, u and v are the velocity components

$$u = \phi_x, \quad v = \phi_y$$

and a is the local speed of sound determined from the energy equation and the stagnation speed of sound

$$a^2 = a_o 2 - (\frac{\gamma-1}{2}) (u^2 - v^2)$$

Solutions are obtained by Jameson's finite difference scheme, reference 4.

AIRFOIL PROFILE REPRESENTATION

Basic Airfoil

Ordinates for the basic NACA 64_1-212 airfoil were approximated by four cubic chain polynomials in the manner of Hicks

$$y_j = a_{o_j} F_1 + a_{1_j} x + a_{2_j} x^2 + a_{3_j} x^3; \quad j = 1,2,3,4$$

Coefficients in the four polynomial arcs are selected on the following

4

$\underline{i = 1}$ - Arc represents forward portion of upper surface

$$F_1 = \sqrt{x}$$

$\underline{i = 2}$ - Arc represents aft portion of upper surface

$$F_2 = 1$$

$\underline{i = 3}$ - Arc represents forward portion of lower surface

$$F_3 = \sqrt{x}$$

$\underline{i = 4}$ - Arc represents aft portion

$$F_4 = 1$$

The coefficients a_{i_j} are determined by introducing four boundary conditions on the airfoil profile in each of the four airfoil arcs. Crout's method for triangularization and back substitution of the resulting systems of linear simultaneous equations. Note that if four points are specified on the aft portion (i = 2 or 4), a discontinuity in slope occurs where the polynomials join. This produces a small ripple in the pressure distribution at the juncture point. However, since the juncture occurs at a region of small slope (x = .5) the effect is not significant. The approximate NACA 64_1-212 airfoil developed by this method is presented in Figure 1.

Additional Thickness

In the present study additional thickness is limited to the upper airfoil surface. The additional thickness has the form

$$\Delta y(x) = \bar{y} \left[1 - \left(\frac{\bar{x}-x}{\bar{x}} \right)^2 \right] ; \quad x < \bar{x}$$

$$\Delta y(x) = \bar{y} \left[1 - \left(\frac{\bar{x}-x}{1-\bar{x}} \right)^2 \right] ; \quad x \geq \bar{x}$$

These functions are of second-order ranging parabolically with $\zeta = |x-\bar{x}|$. Additional thickness is zero at the ending edge (x=0) and trailing edge (x=1) and has a maximum of $\Delta y=\bar{y}$ at $x=\bar{x}$. Additional thickness and slope of the additional thickness are continuous throughout the interval $o < n < 1$. Second derivative of the additional thickness distribution is constant in the forward and aft airfoil arcs but has a discontinuity at the arc junction, $x=\bar{x}$. It follows that a continuous polynomial representation of the additional

5

thickness distributions, valid in the interval $o < n < 1$ would be in the form of an infinite series. This type of additional thickness distribution is referred to as a "biquadratic" function in recognition of the above characteristics. A sequence of biquadratic arcs having varying maximum thickness positions are presented in Figure 2.

PRESENTATION OF RESULTS

Additional Thickness Optimization

Lift Coefficient Maximization

Maximization of lift coefficient has the form

$$\emptyset = \text{Max} \left[C_L \right]$$

where

$$C_L = \oint \Delta p(x) dx$$

and the integration is around the airfoil contour. Since the airfoil contour is completely described in terms of the two parameters $\bar{x}$ and $\bar{y}$

$$\emptyset = \text{Max} \left[C_L \right] = \text{Max} \left[C_L(\bar{x}, \bar{y}) \right]$$

where

$$\bar{x}_L \leq \bar{x} \leq \bar{x}_M$$

$$\bar{y}_L \leq \bar{y} \leq \bar{y}_M$$

This two variable multivariable search problem was solved by a combination of directed random-ray and pattern searches, Ref. 3. Table I presents the results of 30 iterations using these search procedures. Lift gains are produced at 27 of the 30 iterations and continue to be made at the computation termination.

Optimization has moved the position of maximum thickness to the most rearward position allowed, $\bar{x} = 0.9$. At termination, lift is increasing monotonically with increasing thickness, $\bar{y}$. Based on this isolated result lift is maximized for additional thickness of the form assumed by moving the position of maximum additional thickness as far aft as allowed and introducing as much additional thickness as allowed.

6

Moment Minimization

Minimization of the moment coefficient has form

$$\emptyset = \text{Min} \left[C_M \right]$$

where

$$C_M = \oint (x - \tfrac{1}{4}) \, \Delta p(x) dx$$

This minimization resulted in a solution directly opposed to lift maximization. The position of maximum thickness moved to the forward face and the amount of additional thickness was minimized. That is, the basic NACA 64,-212 airfoil has less adverse moment than any airfoil generated by addition of biquadratic thickness to the upper surface of the airfoil.

Lift vs. Moment Trade

Preliminary work using other airfoil thickness representations has indicated that the requirements of lift maximization and moment minimization oppose each other. This is confirmed by the results reported above. It has been found as a result of previous studies that it is very difficult to produce an airfoil for which

$$C_M < .177 - .22 \, C_L$$

This function has been used to define airfoil which have favorable lift/moment characteristics by solution of the problem

$$\emptyset = \text{Min} \left[.177 - .22 \, C_L - C_M \right]$$

Solution of this problem by directed random-ray and pattern search indicates that additional thickness should be added as far forward as possible and that maximum amount of additional thickness should be employed.

Optimization Summary

Three optimal airfoil results have been obtained consistent with the class of airfoil profiles considered here. These results are summarized in Table II. It can be seen that in all cases the position of maximum thickness, $\bar{x}$, is either at the extreme forward or rearward position allowed. Similarly, depending on problem specification, the amount of additional

...ness is either minimized or maximized. The low dimensionality of this problem (two parameters, $\bar{x}$ and $\bar{y}$) permit a ready mapping of these results as a function of $\bar{x}$ and $\bar{y}$. This is done in the following section.

SYSTEMATIC VARIATION OF
AIRFOIL SHAPING PARAMETERS

A systematic investigation on the effect of variations in the airfoil shaping parameters $\bar{x}$ and $\bar{y}$ was undertaken. The resulting airfoils and calculated pressure distributions are presented in Figures 3(a) to 3(v). It should be noted that the airfoils are not drawn to scale in Figure 3. To emphasize profile characteristics the vertical scale is exagerated. The pressure signatures vary in a radical manner with $\bar{x}$ and $\bar{y}$. The basic airfoil exhibits a sharp pressure peak at the leading edge. The magnitude of the peak pressure is reduced by introducing additional thickness in a forward location, $\bar{x} = .1$, and the peak position moves aft. However, if the amount of additional thickness is increased the pressure peak magnitude again increases. This peak is well aft of the leading edge. This effect persists until rearward locations of $\bar{x}$ are encountered. For example, introducing additional thickness at $\bar{x} = .8$ results in a rearward "hump" in the pressure distribution. The increased circulation produced by this hump results in an increased leading edge peak in the airfoil pressure distribution. Flow separation would probably be encountered with these rearward additional thickness distributions unless devices such as rotating cylinders or blowing were employed.

Figure 4 illustrates the effect of varying position of maximum thickness and maximum thickness on lift coefficient. It can be seen that lift coefficient is maximized by increasing both $\bar{x}$ and $\bar{y}$. This confirms optimization studies in the previous section. Since the additional thickness and the basic 12% airfoil thickness are additive Figure 3 presents lift coefficient as a function of thickness. To first-order the airfoil thickness required is

$$t/c = 12\% + \bar{y}$$

8

As it moves to the extremes of the range the actual airfoil thickness is less than this amount as the positions of maximum thickness on the basic and additional thickness distributions are significantly different.

Moment coefficient variation with $\bar{x}$ and $\bar{y}$ is presented in Figure 5. It can be seen that the increased lift available from additional thickness is accompanied by an increase in undesirable pitching moment coefficient. The conclusion of the previous section that moment coefficient is minimized by moving $\bar{x}$ forward and diminishing $\bar{y}$ is borne out by Figure 5, again confirming the optimization study results.

A final verification of the optimization procedures employed is provided by Figure 6. Here the variation of C_M and C_L with $\bar{x}$ and $\bar{y}$ is presented together with the line function

$$.177 - .22\, C_L - C_M = 0$$

It can be seen that based on this function the most favorable $C_M - C_L$ trade involves moving $\bar{x}$ forward and introducing the maximum $\bar{y}$.

Figure 7 presents the relationship between pressure peak and lift coefficient for a range of $\bar{x}$ and $\bar{y}$ values. For each value of $\bar{y}$ (maximum additional thickness) there is a point at which the pressure peak magnitude is minimized. Cross plotting the peak pressures as a function of C_L in Figure 8 reveals the minimum peak pressures as a function of C_L.

Figure 9 plots the position of maximum additional thickness as a function of C_L. As C_L increases $\bar{x}$ moves aft. The associated values of $\bar{y}$ required for the low peak pressure is also plotted in Figure 9. Finally, Figure 10 plots the minimum C_p attainable as a function of C_L using the biquadratic additional thickness airfoil model.

CONCLUSION

A numerical investigation into a class of modified airfoil shapes has been completed using full two-dimensional flow potential flow equations. Airfoils studied were obtained by modifying the NACA 64_1-212 airfoil by additional thickness distributions based on a biquadratic variation with

9

chordwise position. Free streamwise Mach number was held constant at
M = 0.2 and the basic airfoil is held at 6° angle-of-attack. Results
of the study may be summarized as follows:

1. Significant changes in pressure distribution, lift and
    pitching moment can be introduced by the biquadratic
    thickness modification.

2. The requirements for improving lift and moment co-
    efficient characteristics are directly opposed to each
    other. That is, increases in lift result in increases
    in adverse moment. Conversely, decreases in adverse moment
    produce decreases in lift.

3. High lift airfoils require the addition of a thickness
    distribution biased to the rear of the foil and as much
    thickness addition as possible.

4. Low adverse moments require a thickness distribution
    biased to the front of the foil and as little additional
    thickness as possible. Therefore, the best airfoil based
    on moment considerations is the unmodified foil.

5. Favorable lift/moment trade-off characteristics are obtained
    by a thickness distribution biased to the front of the foil
    employing as much thickness as possible.

6. There exists a class of airfoil exhibiting low peak pressures
    for a given C_L which require an intermediate location of
    maximum additional thickness and thickness amount. Generally,
    the position of maximum additional thickness moves to the
    rear with increasing C_L, and the amount of additional thickness
    required increases with increasing C_L.

TABLE I

CONVERGENCE FOR C_L MAXIMIZATION

			$\bar{x}$	$\bar{y}$	$-C_L$
M	C	JJJ	ALPHA(1)	ALPHA(2)	FUNCTN(1)
0	1	1	.2500	1.0000E-03	-.8941
10	1	2	.2508	1.0365E-03	-.8942
10	1	3	.2583	1.1667E-03	-.8952
10	1	5	.2626	1.4155E-03	-.8968
2	1	6	.2753	1.8311E-03	-.8982
2	1	7	.2879	2.2466E-03	-.9022
2	1	8	.3132	3.0776E-03	-.9078
2	1	9	.3638	4.7398E-03	-.9196
10	2	10	.3688	4.7533E-03	-.9198
10	2	11	.3758	5.2172E-03	-.9216
10	2	12	.3824	5.5611E-03	-.9258
2	2	13	.4010	6.3824E-03	-.9320
2	2	14	.4196	7.2037E-03	-.9385
2	2	15	.4567	8.8462E-03	-.9520
2	2	16	.5311	1.2131E-02	-.9826
10	3	17	.5505	1.2761E-02	-.9863
10	3	18	.5675	1.2812E-02	-.9920
10	3	20	.5808	1.3494E-02	-.9993
2	3	21	.6305	1.4856E-02	-1.018
2	3	22	.6802	1.6219E-02	-1.041
2	3	23	.7796	1.8944E-02	-1.105
2	3	24	.9000	2.4394E-02	-1.303
10	4	25	.9000	2.5016E-02	-1.313
10	4	26	.9000	2.7157E-02	-1.350
10	4	27	.9000	3.0116E-02	-1.399
2	4	28	.9000	3.5838E-02	-1.493
2	4	29	.9000	4.1560E-02	-1.586
2	4	30	.9000	5.3003E-02	-1.765

TABLE II

OPTIMAL AIRFOIL SHAPING RESULTS

Problem	Maximum Thickness Position	Thickness
Max C_L	Aft	Max.
Min C_M	Forward	Min.
Min C_M/C_L Trade	Forward	Max.

64(1)-212 AIRFOIL AND PRESSURE DISTRIBUTION
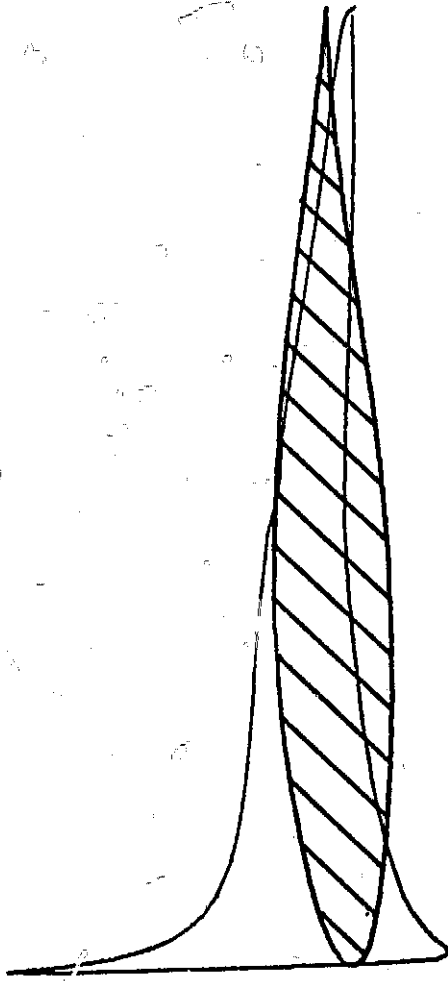
FIGURE 1
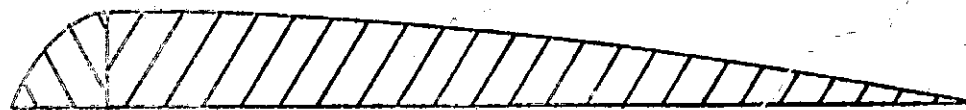
a) $\bar{x} = .1$

b) $\bar{x} = .3$

c) $\bar{x} = .5$

d) $\bar{x} = .7$

e) $\bar{x} = .9$

FIGURE 2   BIQUADRATIC ADDITIONAL THICKNESS DISTRIBUTIONS

14

64(1)-212 EXTENSION X = .1 , Y = .06

ACTUAL AIRFOIL IS 18% THICK
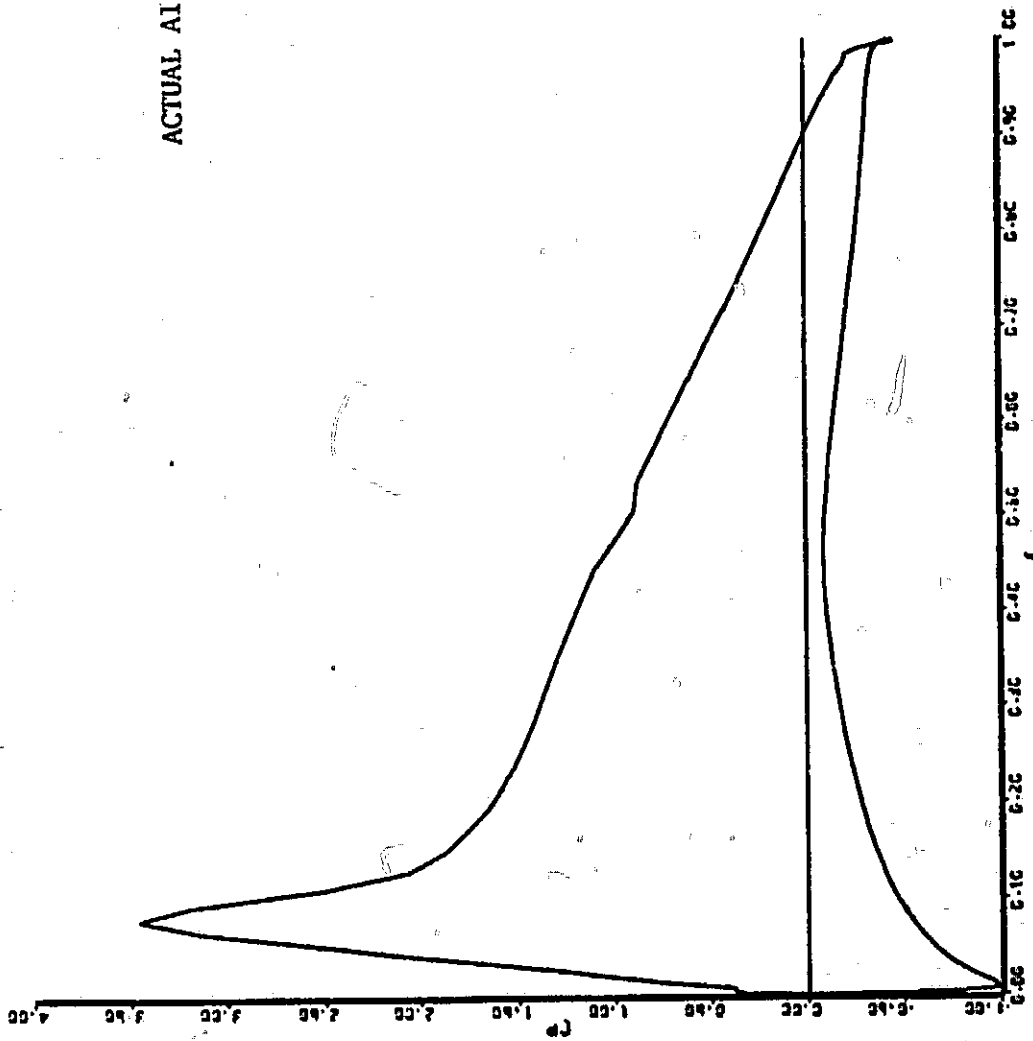
FIGURE 3(a)

64111-212 EXTENSION X = .1 Y = .09

ACTUAL AIRFOIL IS 21% THICK

FIGURE 3(b)

16
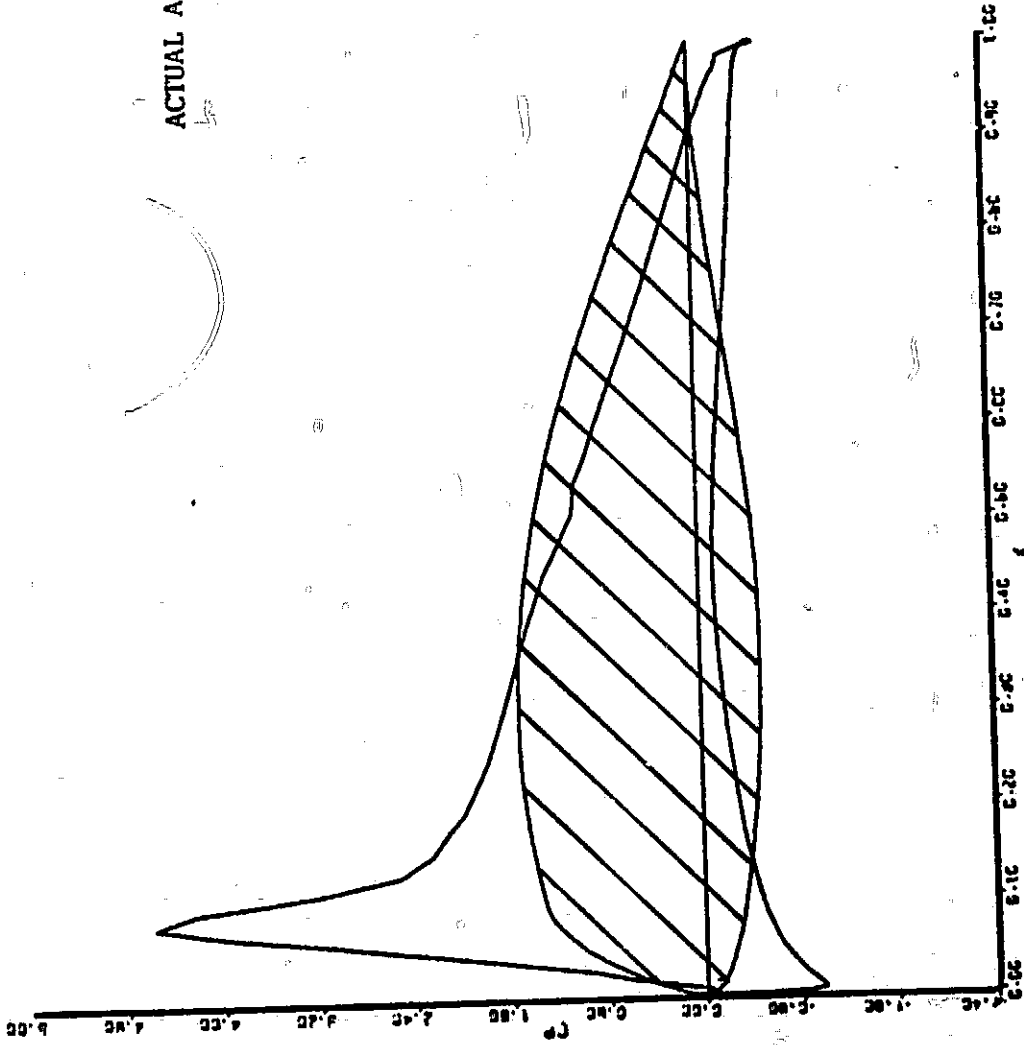
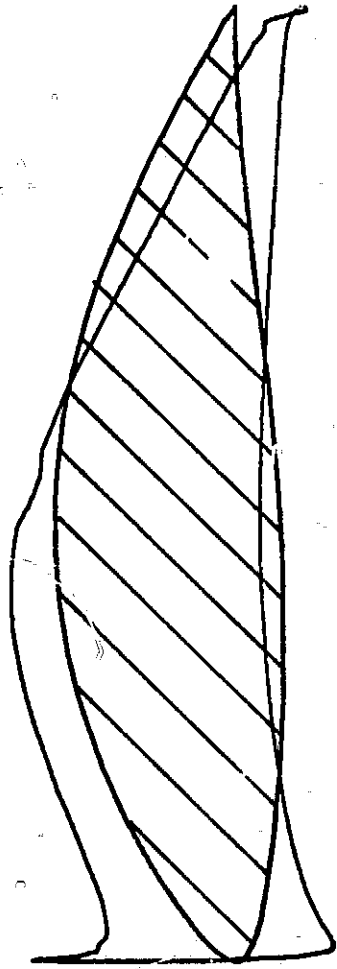64⌐11-212 EXTENSION X=.2 Y=.03
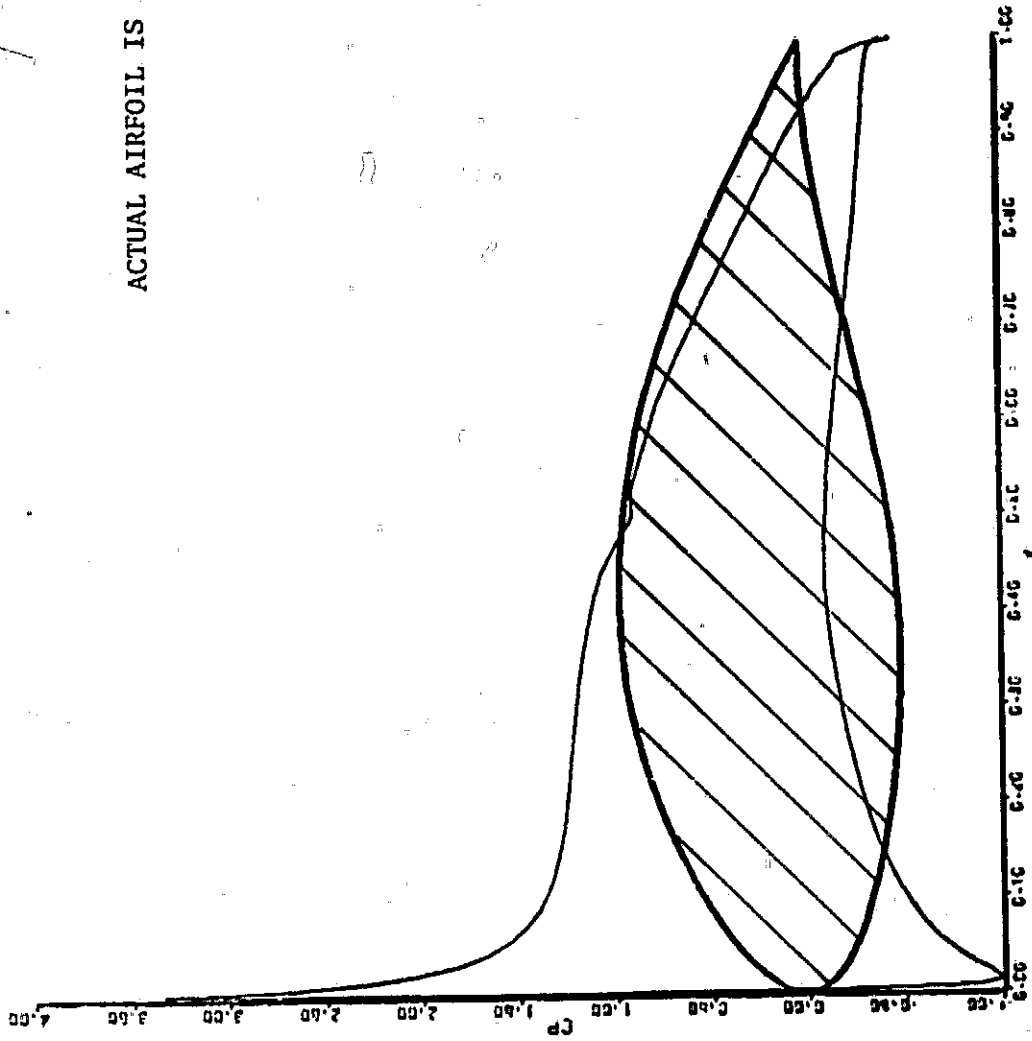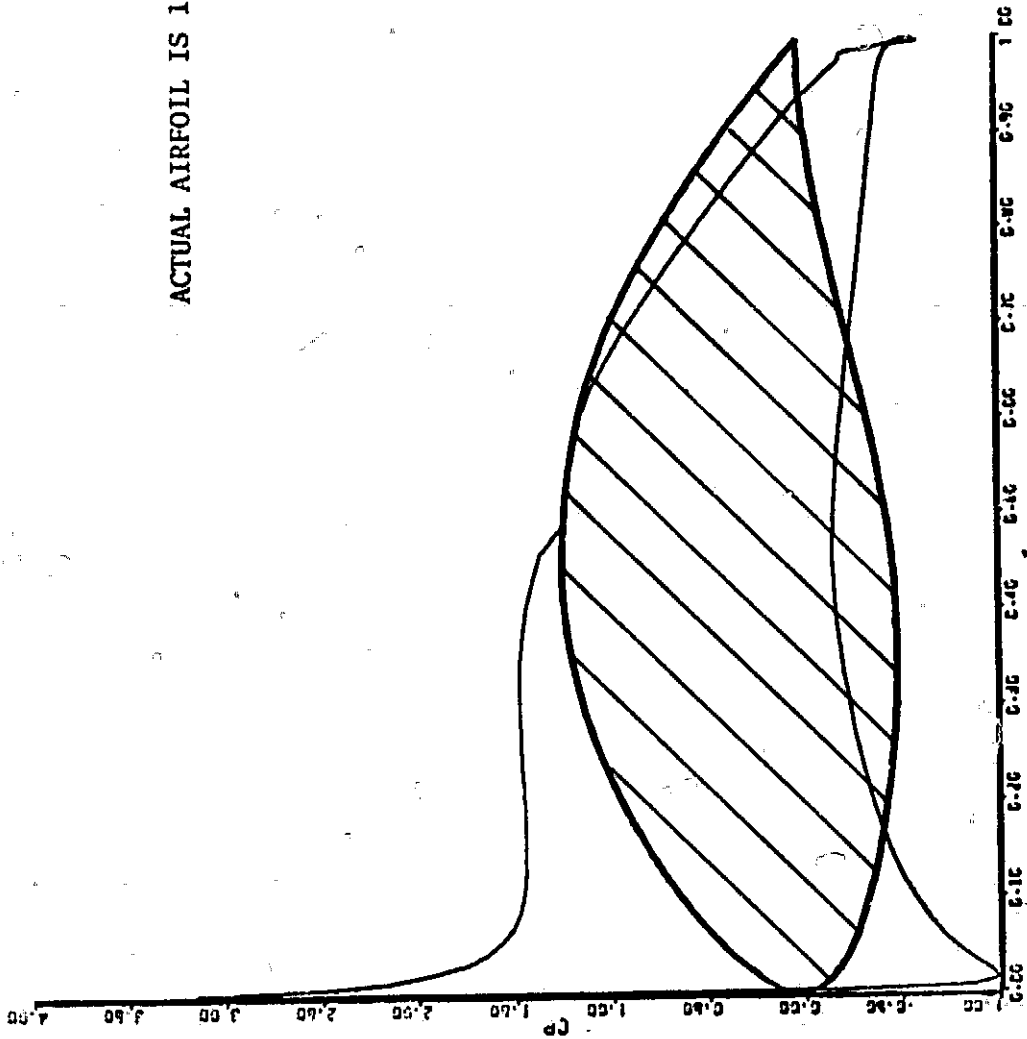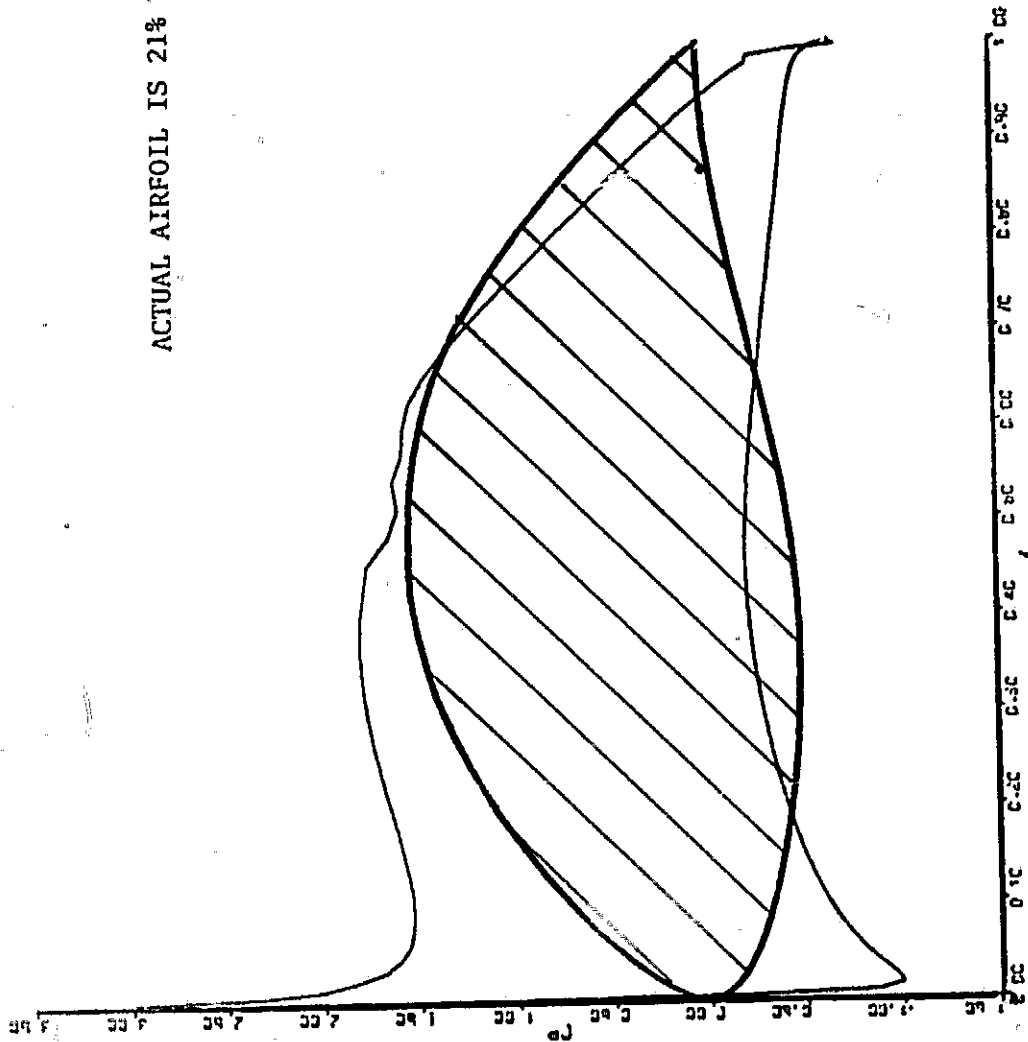
ACTUAL AIRFOIL IS 15% THICK
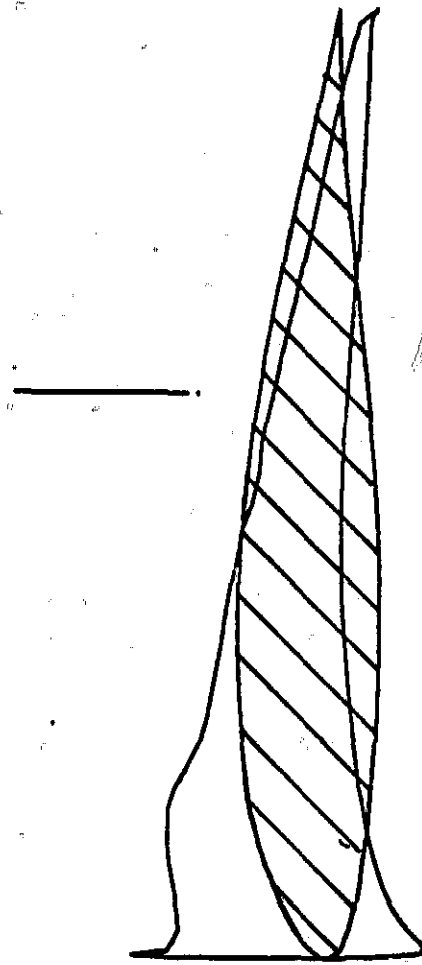
FIGURE 3(c)

64(11-212 EXTENSION X=.2 Y=.06

ACTUAL AIRFOIL IS 18% THICK
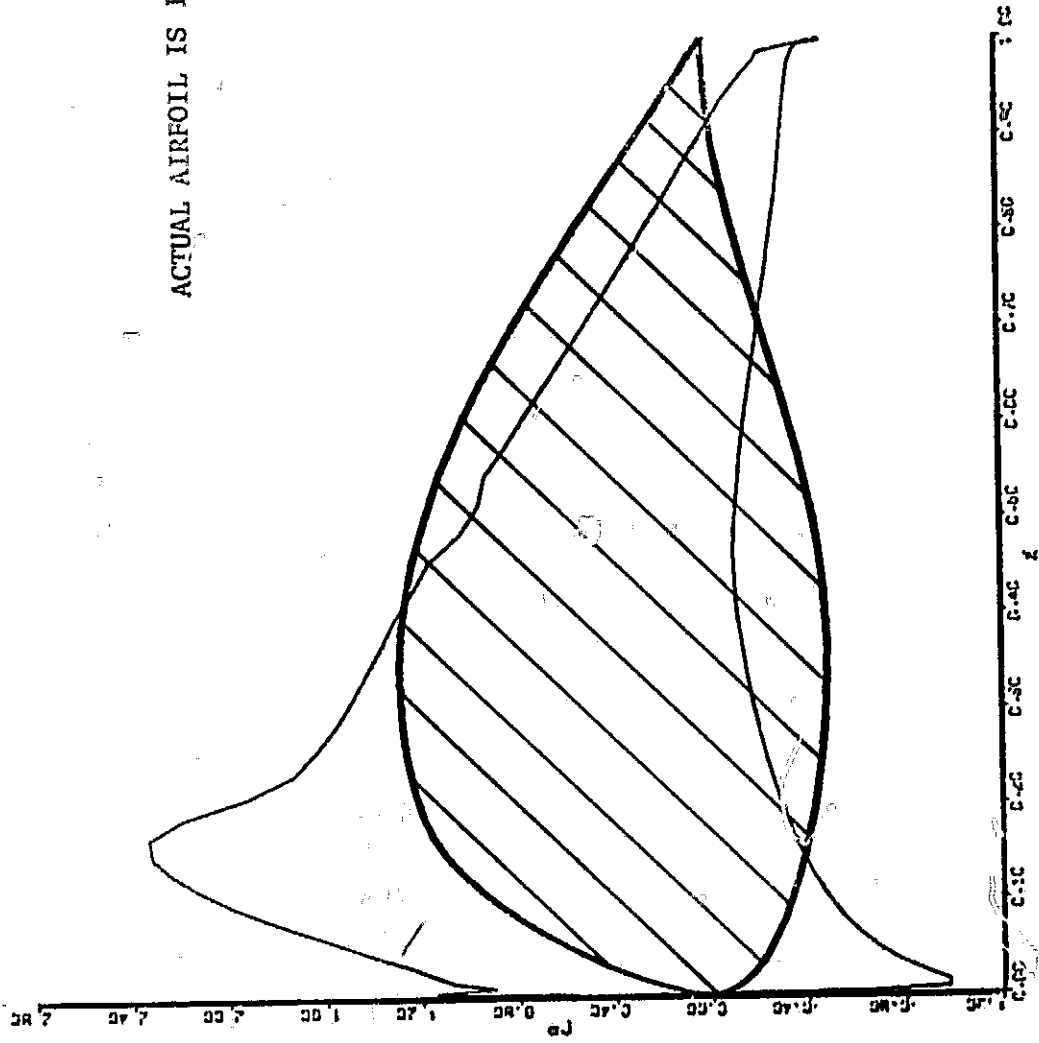
FIGURE 3(d)

64(11)-212 EXTENSION X=.2 Y=.09

ACTUAL AIRFOIL IS 21% THICK
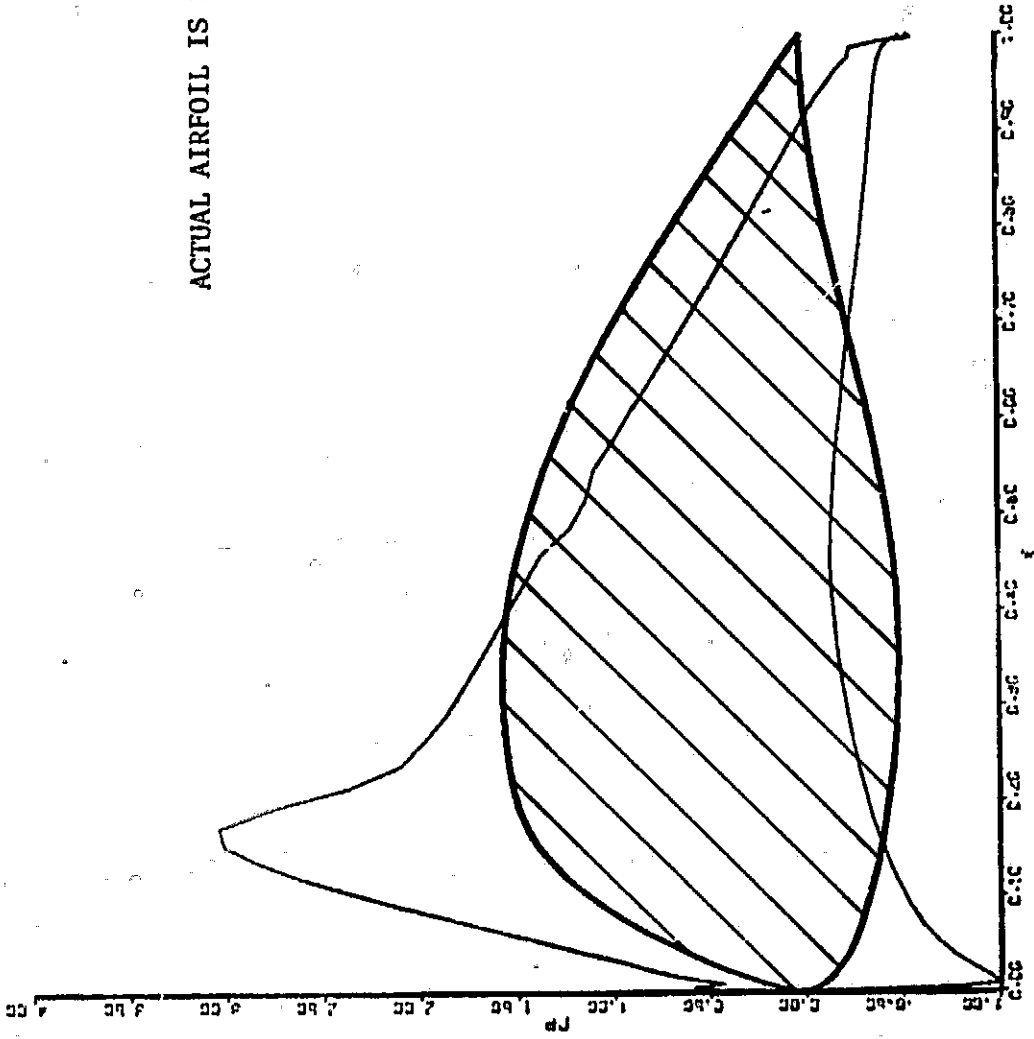
FIGURE 3(e)

64(1)-212-EXTENSION X=.2 Y=.12

ACTUAL AIRFOIL IS 24% THICK
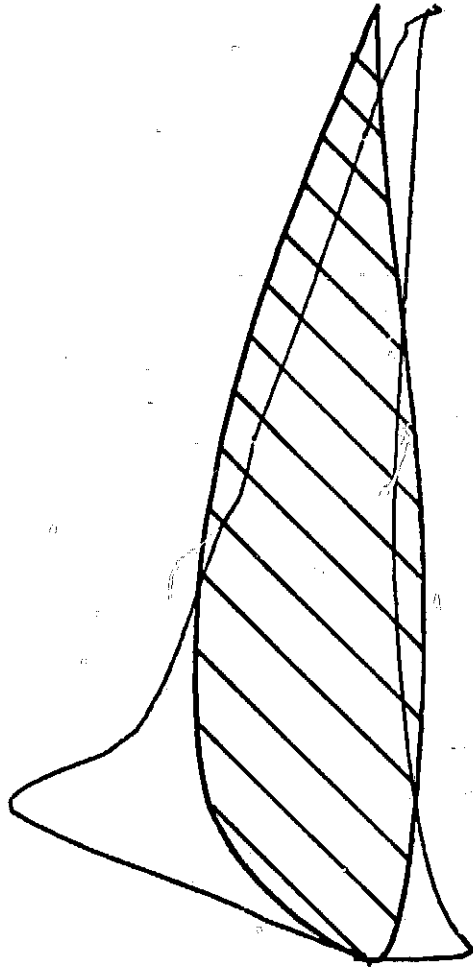
FIGURE 3(f)

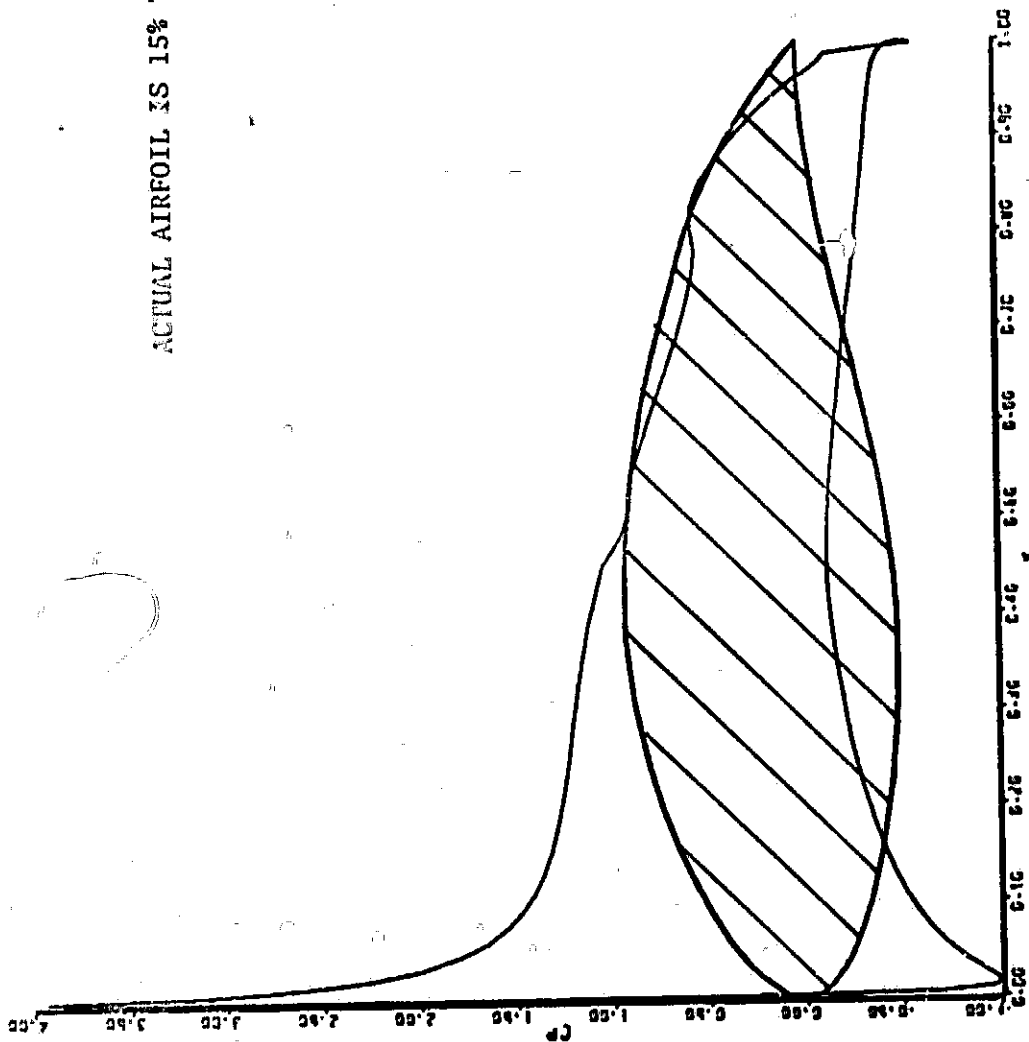G4(11)-212 EXTENSION X=.3 Y=.03

ACTUAL AIRFOIL IS 15% THICK
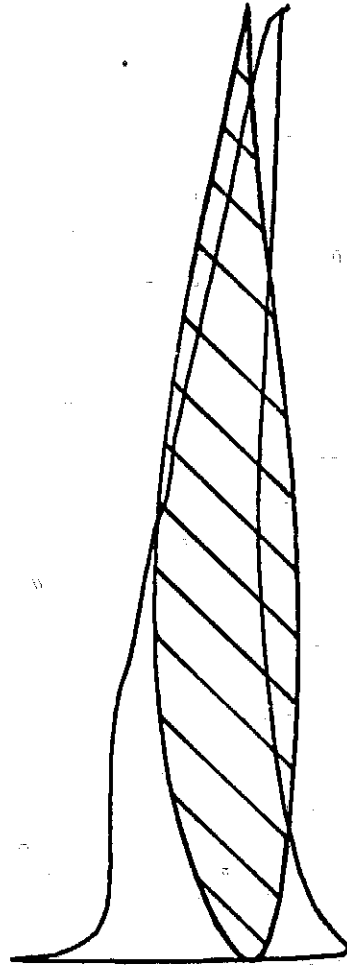
FIGURE 3(g)

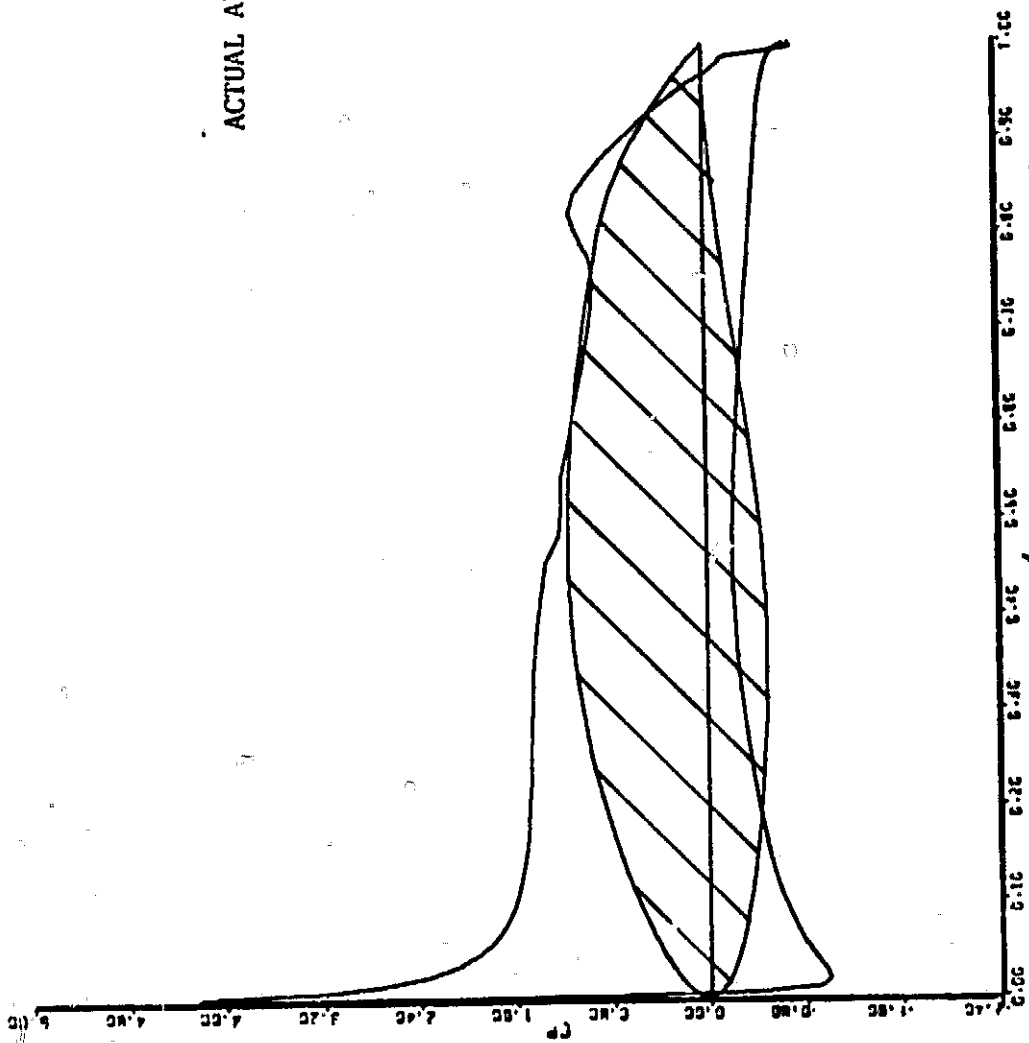64111-212 EXTENSION X=.3 Y=.06

ACTUAL AIRFOIL IS 18% THICK
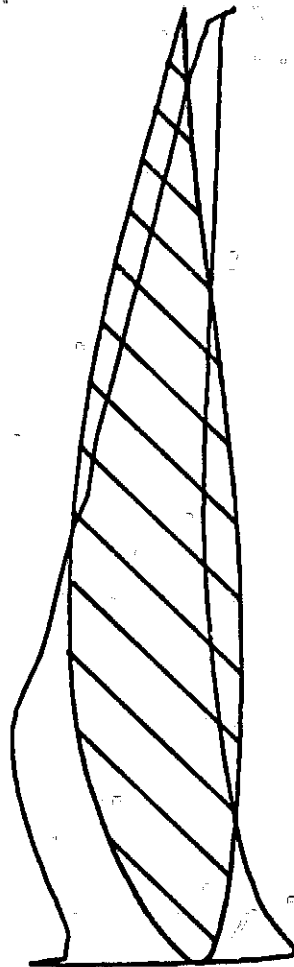
FIGURE 3(h)

64(1)1-212 EXTENSION X=.3 Y=.09

ACTUAL AIRFOIL IS 21% THICK

FIGURE 3(i)

23
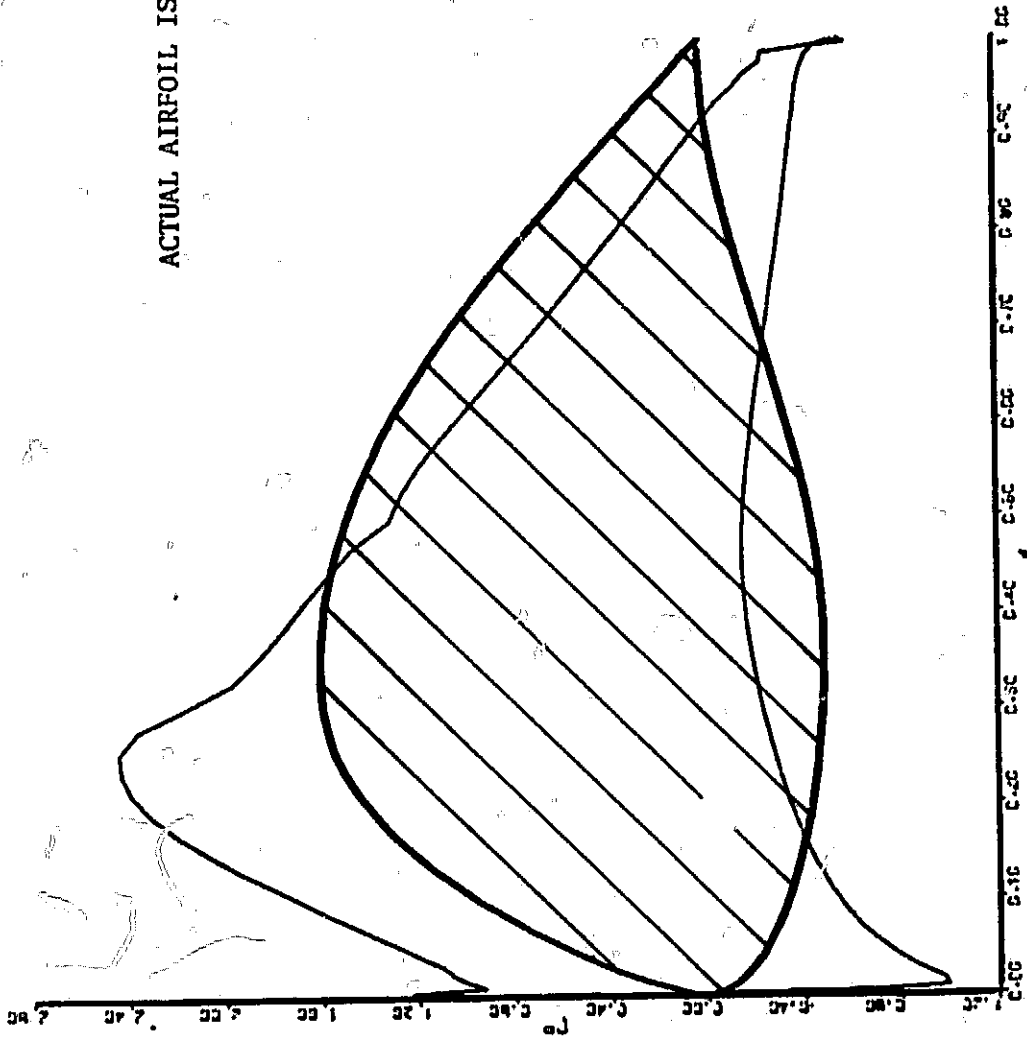
64.(1)-062 EXTENSION X=.4 Y=.03

ACTUAL AIRFOIL IS 15% THICK

FIGURE 3(j)

24
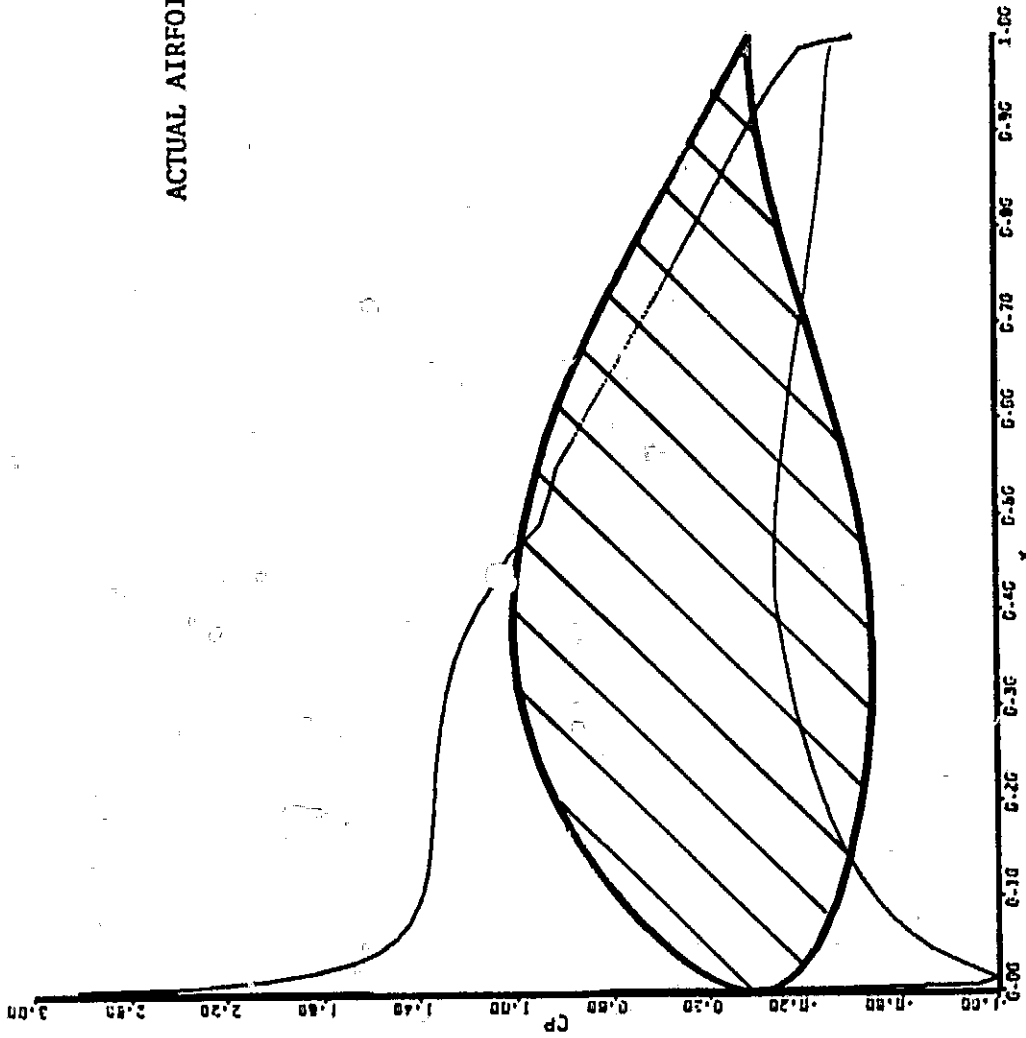
64(1)-062 EXTENSION X=.4 Y=.06

ACTUAL AIRFOIL IS 18% THICK

FIGURE 3(k)

25
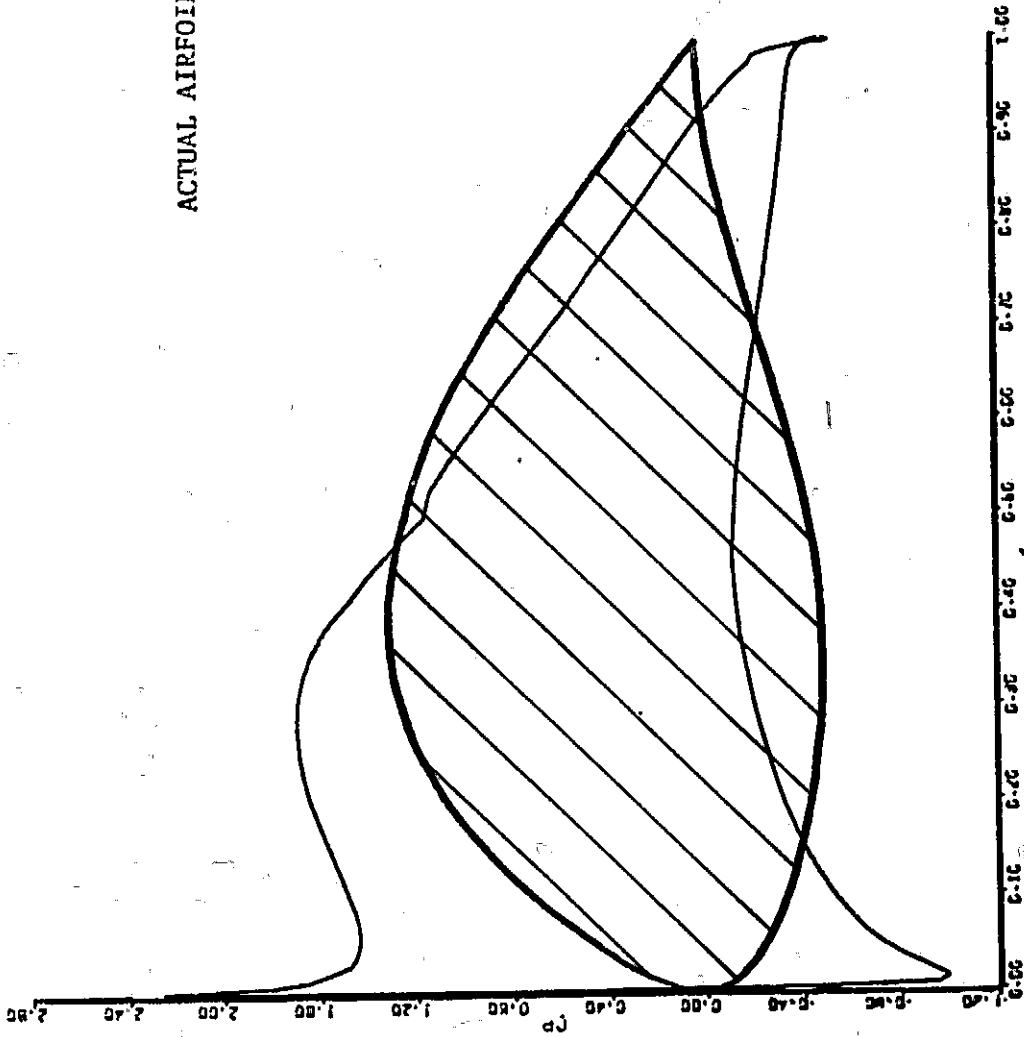
64(1)-062 EXTENSION X=.4 Y=.09

ACTUAL AIRFOIL IS 21% THICK

FIGURE 3(1)

26
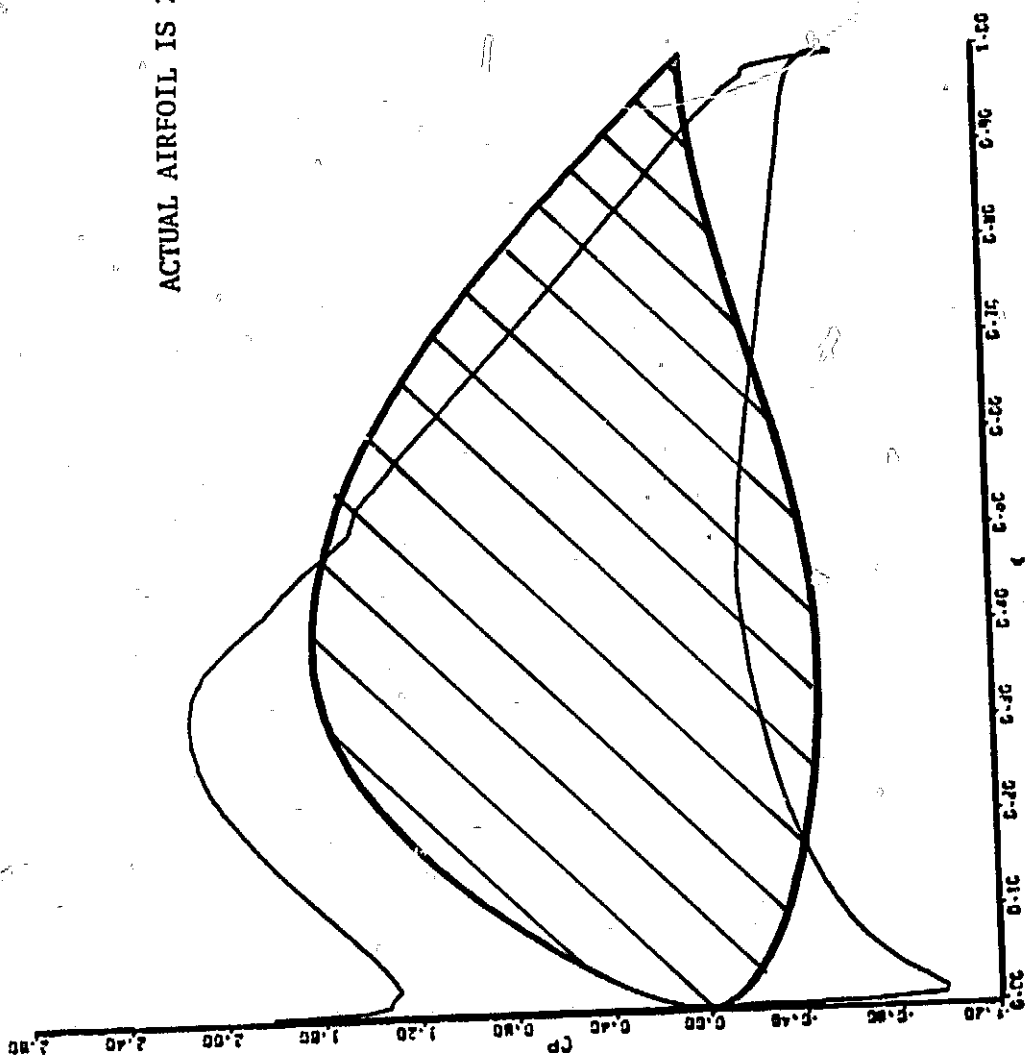
64(1)-212 EXTENSION X=.5 Y=-.03

ACTUAL AIRFOIL IS 15% THICK
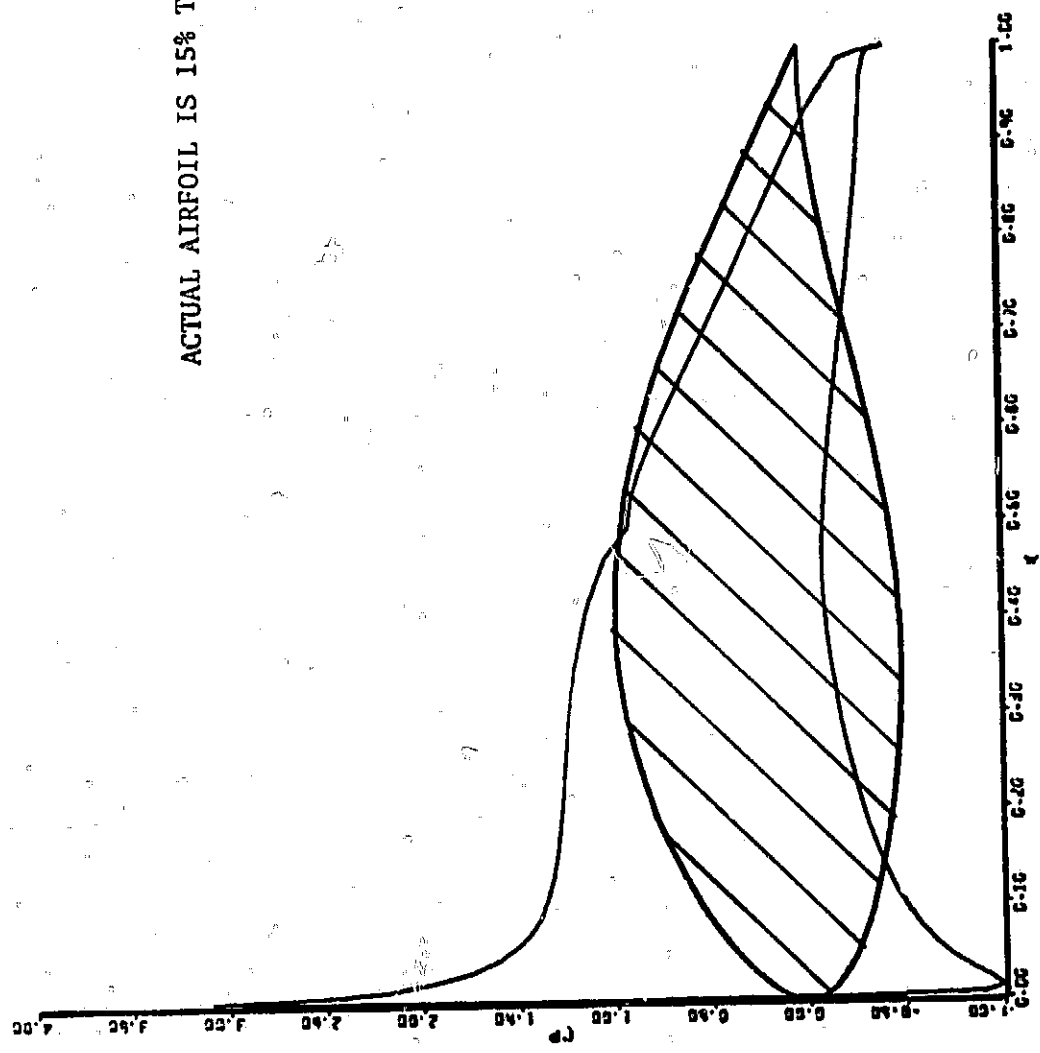
FIGURE 3(m)

64(1)-212 CHECK RUN X=.5 Y=.06

ACTUAL AIRFOIL IS 18% THICK
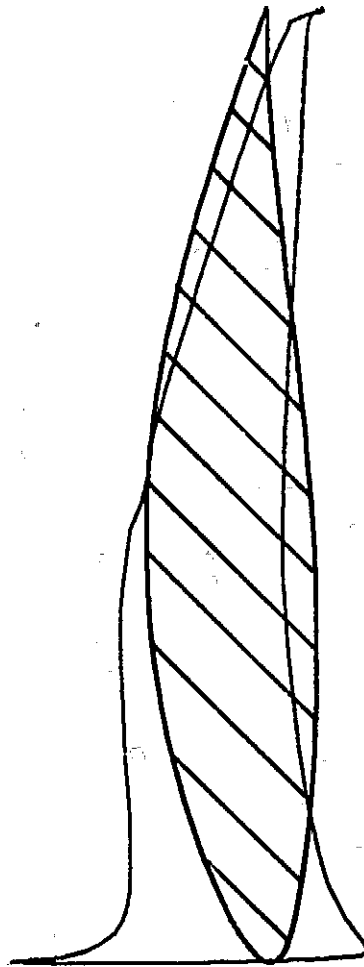
FIGURE 3(n)

64111-212 EXTENSION X = .5 ⅄ = .69

ACTUAL AIRFOIL IS 21% THICK

FIGURE 3(o)

29
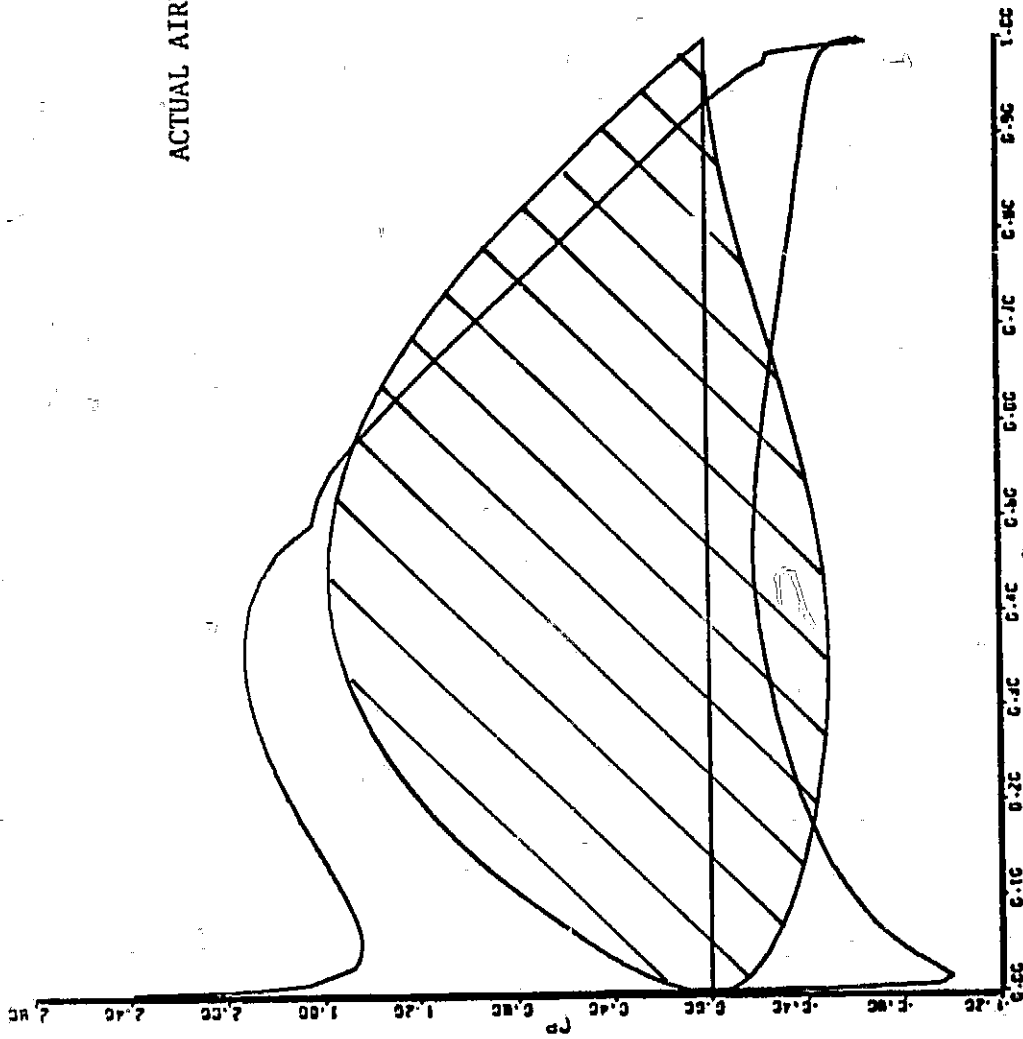
64(1)-212 EXTENSION X=   Y=.12

ACTUAL AIRFOIL IS 24% THICK

FIGURE 3(p)

64(1)-362 EXTENSION X=.6 Y=.03

ACTUAL AIRFOIL IS 15% THICK

CP

FIGURE 3(q)

64(1)-062 EXTENSION X=.6 Y=-.06

ACTUAL AIRFOIL IS 18% THICK

FIGURE 3(r)

64(11-062 EXTENSION X=.6 Y=.09

ACTUAL AIRFOIL IS 21% THICK

Cp

FIGURE 3(s)

64111-212 -EXTENSION X=.8 Y=.03

ACTUAL AIRFOIL IS 15% THICK

FIGURE 3(t)

34

64(1)-2)2 EXTENSION X = .8 Y = .06

ACTUAL AIRFOIL IS 18% THICK

FIGURE 3(u)

64/11-212 EXTENSION X=.8 Y=.09

ACTUAL AIRFOIL IS 21% THICK

FIGURE 3(v)

36

.12
.09
.06
.03
$\bar{y} = 0$

$\bar{x}$

.2   .4   .6   .8

C_L

1.8

1.4

1
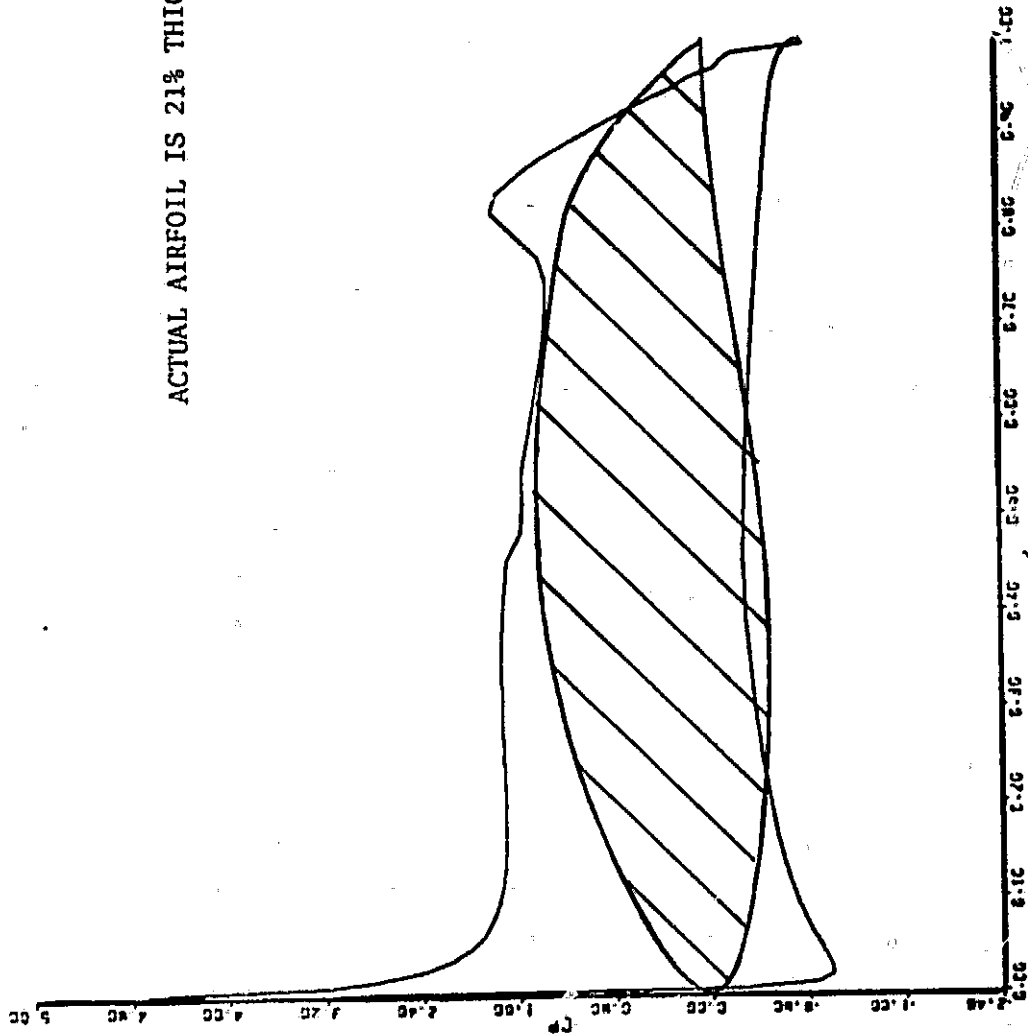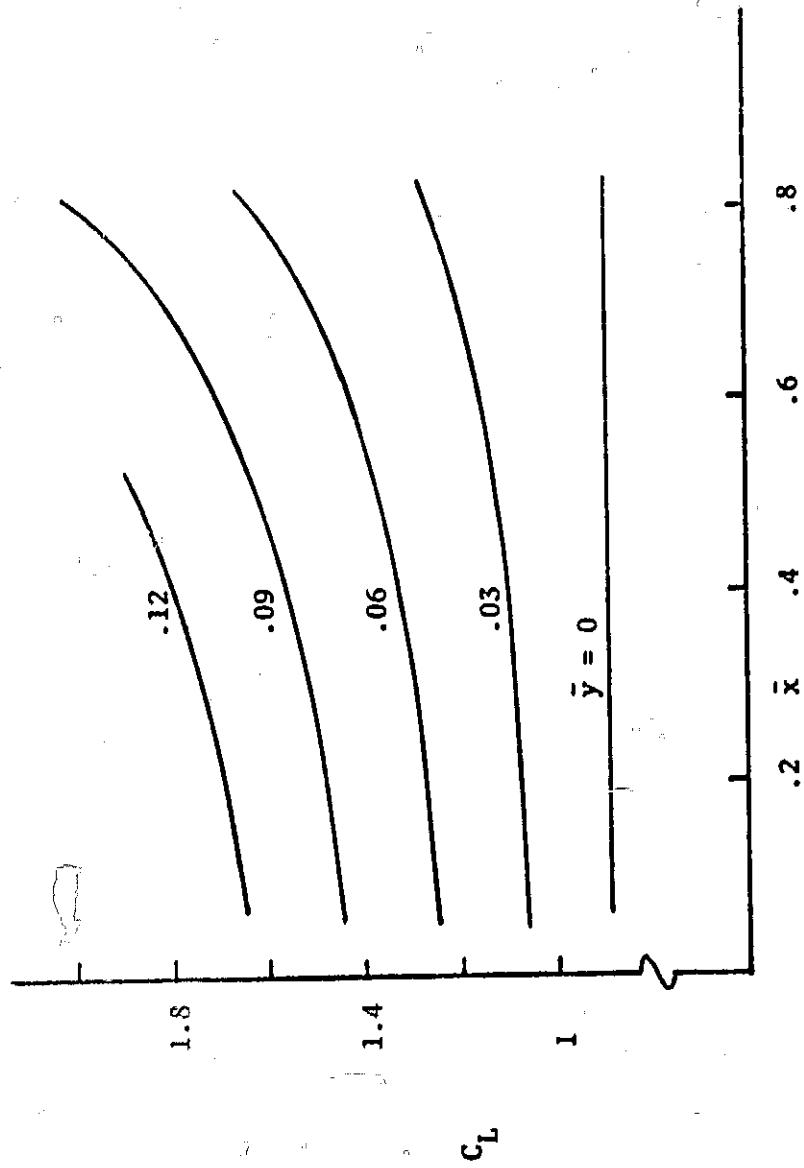
FIGURE 4.   LIFT COEFFICIENT, BIQUADRATIC MODIFICATIONS TO 64_1-212
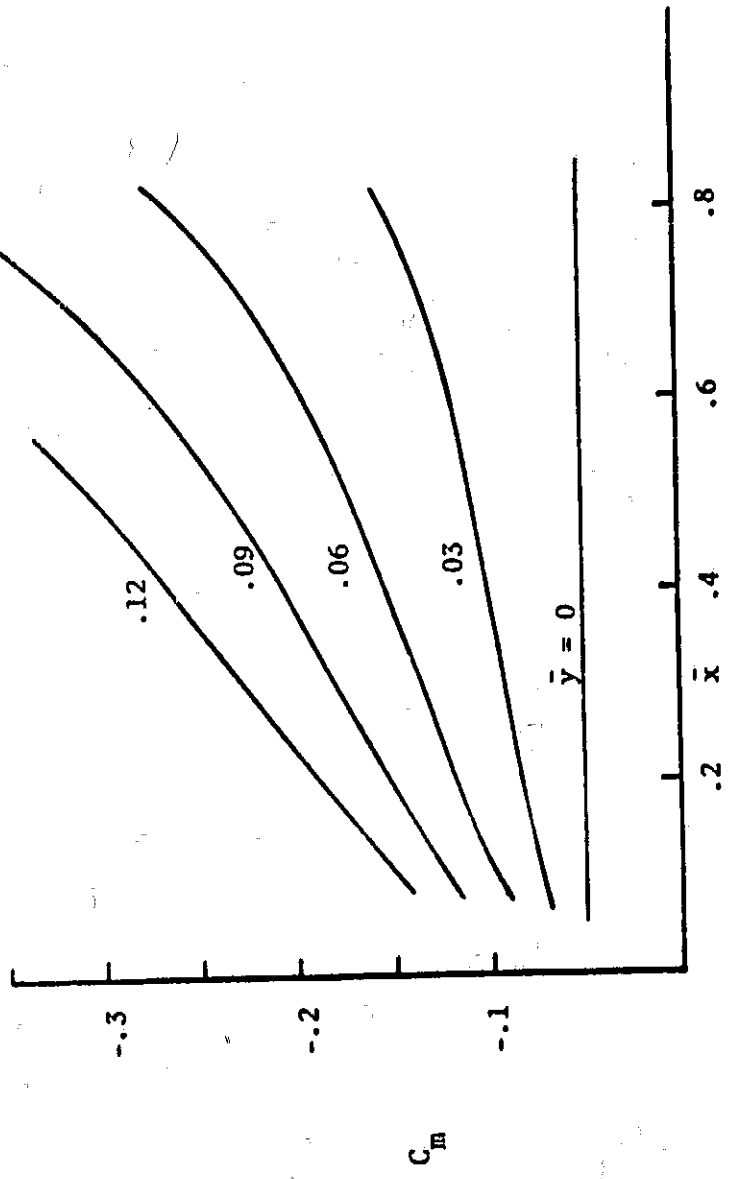
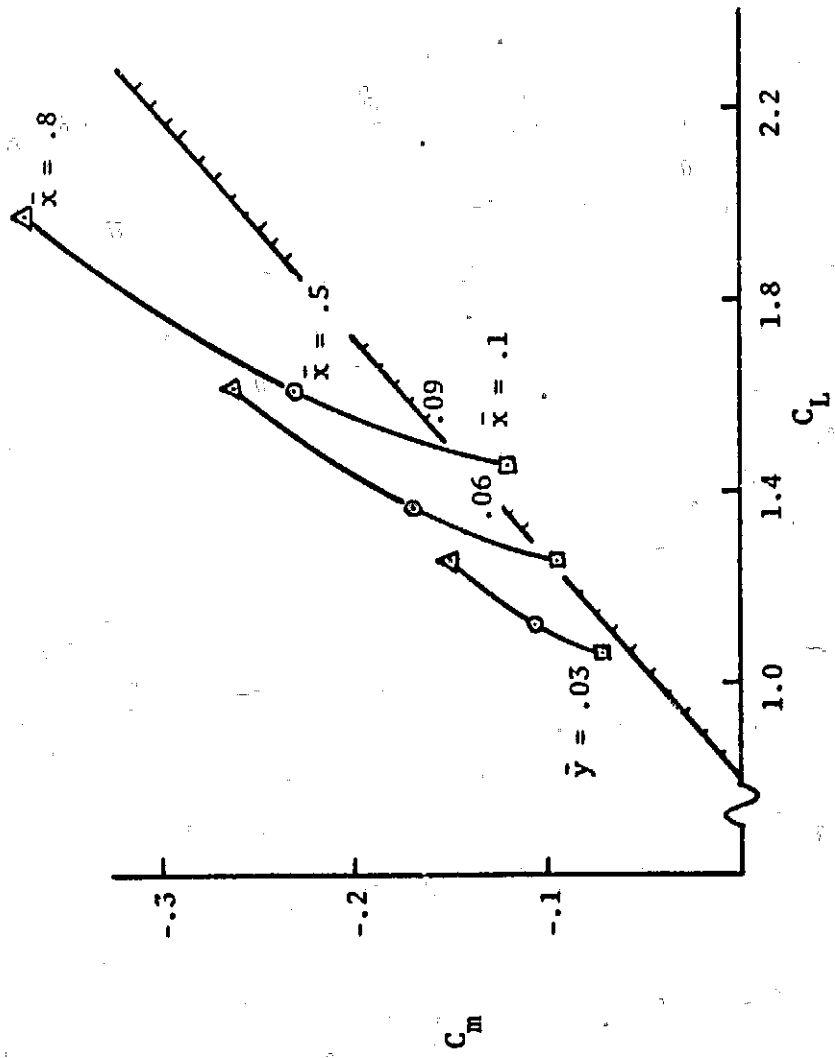FIGURE 5. MOMENT COEFFICIENT, BIQUADRATIC MODIFICATIONS TO 64_1-212
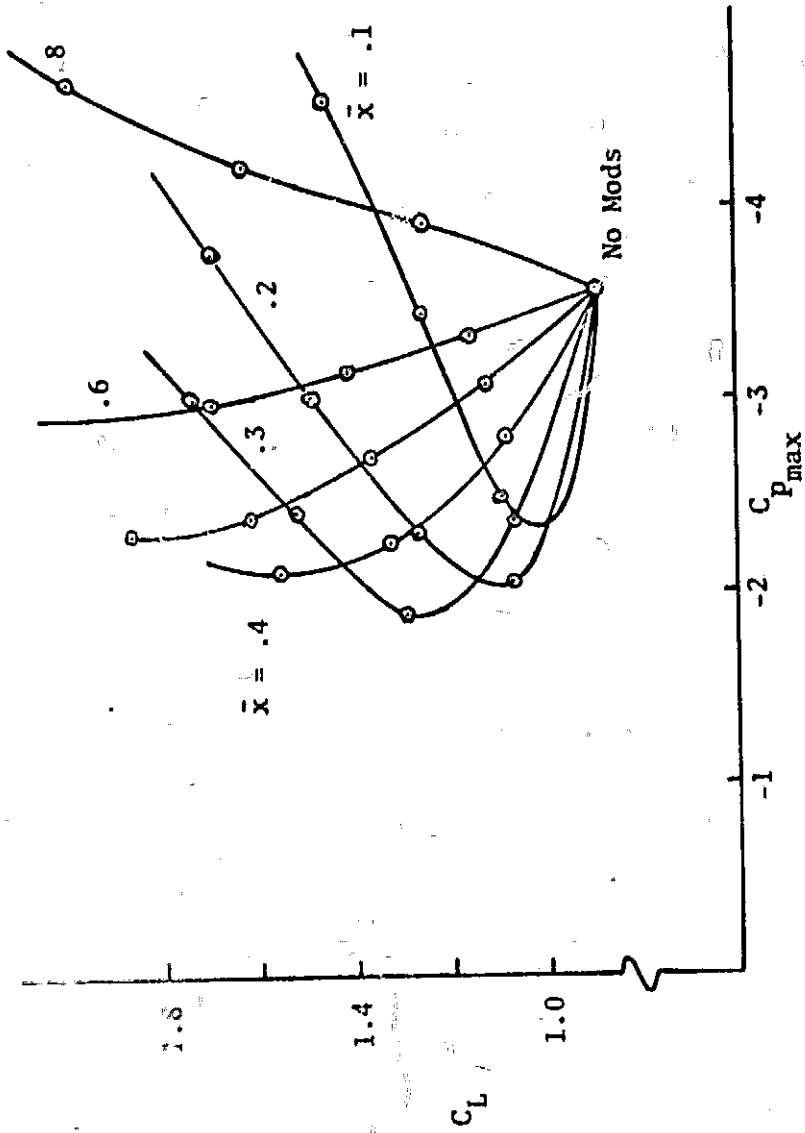
38

FIGURE 6.   LIFT AND MOMENT VARIATIONS
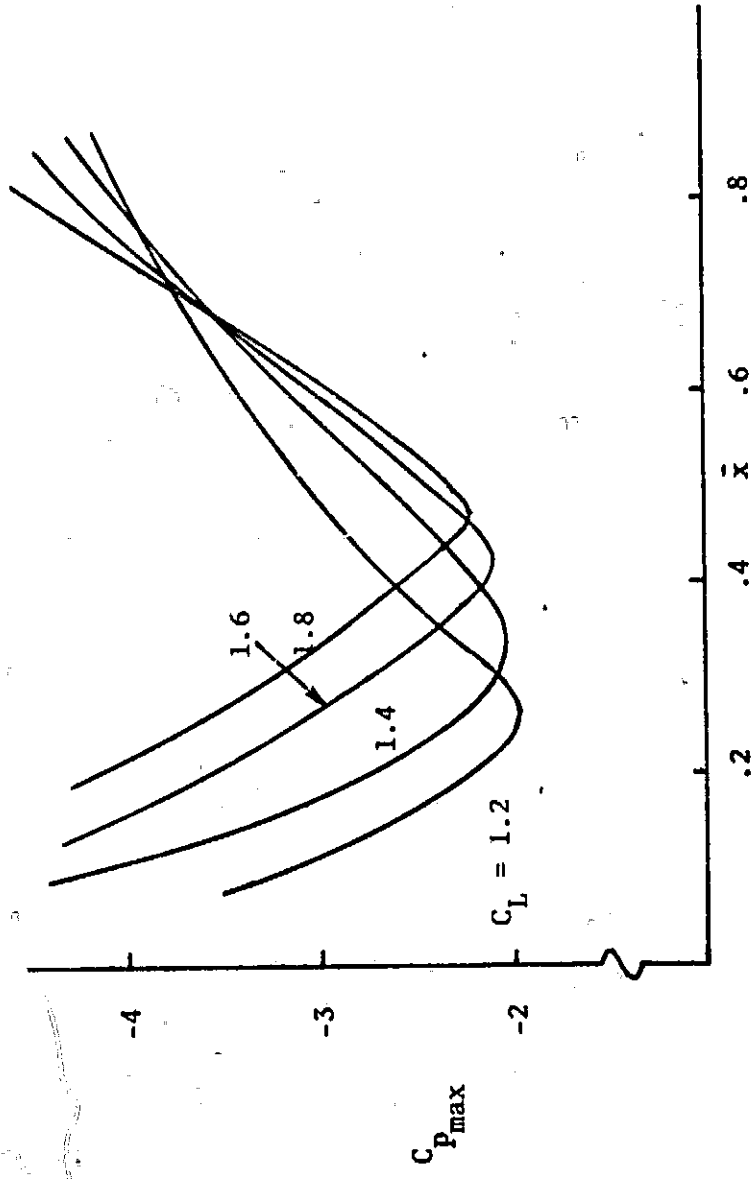
FIGURE 7. BIQUADRATIC MODIFICATIONS TO 64_1-212
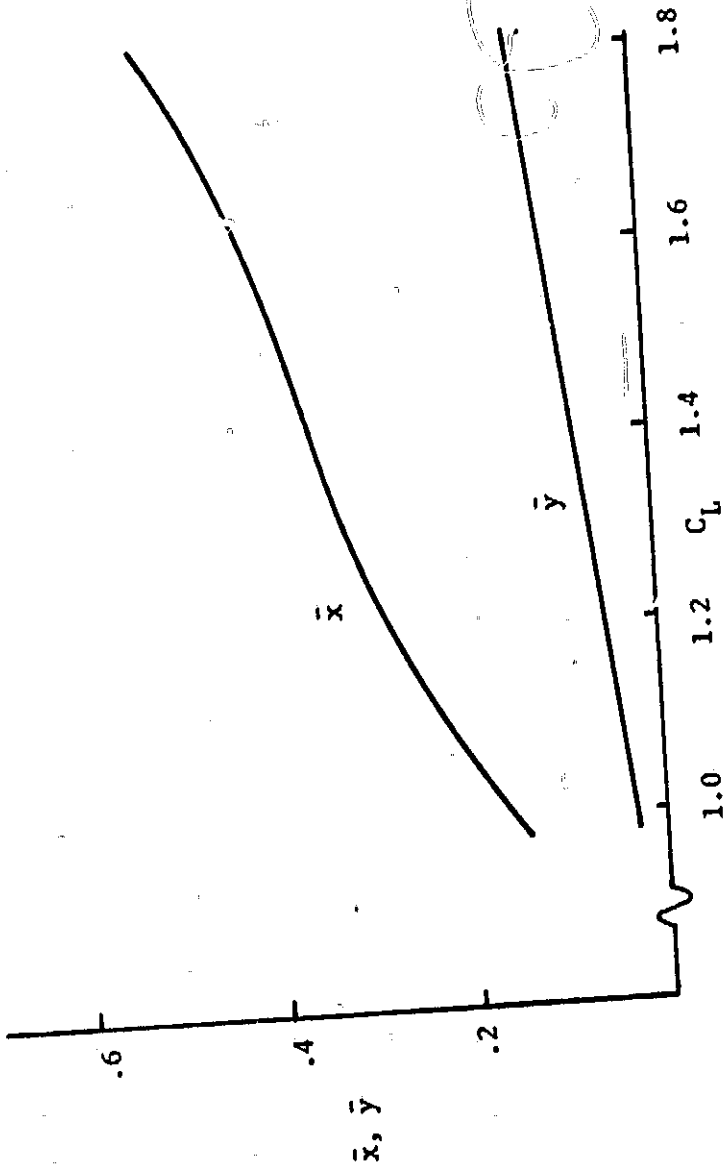
FIGURE 8. BIQUADRATIC MODIFICATIONS TO 64_1-212

FIGURE 9. ADDITIONAL THICKNESS DISTRIBUTION TO MINIMIZE PEAK PRESSURE
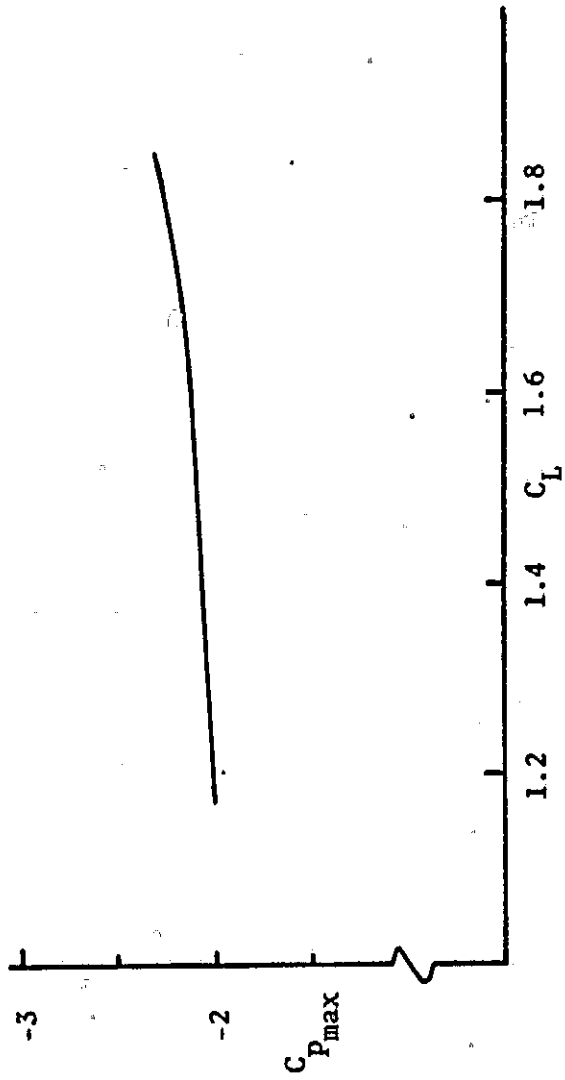
42

FIGURE 10.   MINIMUM PEAK PRESSURE OBTAINABLE WITH BIQUADRATIC MODIFICATIONS

REFERENCES

1. Hicks, R. M., Merman, E. M., and Vanderplaatz, G. N., "Assessment of Airfoil Design by Numerical Optimization," NASA TMX-3092, July 1974.

2. Liebeck, R. H., "A Class of Airfoils Designed for High Lift in Incompressible Flow," J. Aircraft, Vol. 10, No. 10, October 1973.

3. Hague, D. S. and Glatt, C. R., "An Introduction to Multivariable Search Techniques for Parameter Optimization (and Program AESOP)," NASA CR73200, April 1968.

4. Jameson, A. "Transonic Flow Calculations for Airfoils and Bodies of Revolution," Grumman Aerodynamics Report 390-71, December 1971.